Virus Research 230 (2017) 19–28

Contents lists available at ScienceDirect

Virus Research

journal homepage: www.elsevier.com/locate/virusres

Interaction of *Mal de Río Cuarto virus* (*Fijivirus* genus) proteins and identification of putative factors determining viroplasm formation and decay

Gabriela Llauger[a], Luis Alejandro de Haro[a,b], Victoria Alfonso[a,b], Mariana del Vas[a,b,*]

[a] *Instituto de Biotecnología, Instituto Nacional de Tecnología Agropecuaria (IB-INTA), Hurlingham, Argentina*
[b] *Consejo Nacional de Investigaciones Científicas y Técnicas, CONICET, Buenos Aires, Argentina*

ARTICLE INFO

Article history:
Received 4 November 2016
Received in revised form 4 January 2017
Accepted 5 January 2017
Available online 10 January 2017

Keywords:
MRCV
viroplasm
PEST sequence
Reoviridae
Y2H

ABSTRACT

Mal de Río Cuarto virus (MRCV) is a member of the *Fijivirus* genus, within the *Reoviridae* family, that replicates and assembles in cytoplasmic inclusion bodies called viroplasms. In this study, we investigated interactions between ten MRCV proteins by yeast two-hybrid (Y2H) assays and identified interactions of non-structural proteins P6/P6, P9-2/P9-2 and P6/P9-1. P9-1 and P6 are the major and minor components of the viroplasms respectively, whereas P9-2 is an N-glycosylated membrane protein of unknown function. Interactions involving P6 and P9-1 were confirmed by bimolecular fluorescence complementation (BiFC) in rice protoplasts. We demonstrated that a region including a predicted coiled-coil domain within the C-terminal moiety of P6 was necessary for P6/P6 and P6/P9-1 interactions. In turn, a short C-terminal arm was necessary for the previously reported P9-1 self-interaction. Transient expression of these proteins by agroinfiltration of *Nicotiana benthamiana* leaves showed very low accumulation levels and further *in silico* analyses allowed us to identify conserved PEST degradation sequences [rich in proline (P), glutamic acid (E), serine (S), and threonine (T)] within P6 and P9-1. The removal of these PEST sequences resulted in a significant increase of the accumulation of both proteins.

1. Introduction

Mal de Río Cuarto virus (MRCV) is a member of the genus *Fijivirus* in the family *Reoviridae* that causes an important maize disease in Argentina, which is the third-largest corn exporter in the world (Attoui et al., 2011; Lenardón et al., 1998; World of Corn, 2016). The virus is transmitted by delphacid planthoppers in a persistent-propagative manner (Arneodo et al., 2002; de Remes Lenicov et al., 1985). As for other fijiviruses, viral replication and assembly occur in cytoplasmic inclusion bodies called viroplasms, which are composed of viral proteins, nucleic acids, and cellular components of unknown function and identity (Attoui et al., 2011). MRCV has a double-shelled icosahedral capsid with short A- and B-spikes on the particle vertices containing 10 double-stranded RNA (dsRNA) segments that encode 13 putative proteins (Distéfano et al., 2005, 2003, 2002; Firth and Atkins, 2009; Guzmán et al., 2007; Mongelli, 2010).

The MRCV structural proteins (SPs) are proposed to be an RNA-dependent RNA polymerase (P1, Distéfano et al., 2003), A- and B-spike proteins (P2 and P4, respectively; Distéfano et al., 2003, 2002), a major core protein (P3, Distéfano et al., 2009, 2003), a possible helicase (P8, Distéfano et al., 2002), and the major outer capsid protein P10 (Distéfano et al., 2005). In addition, P4 contains an active site for guanylyl transferases (Distéfano et al., 2002; Supyani et al., 2007). On the other hand, MRCV segments S5, S6, S7 and S9 code for non-structural proteins (NSPs) P5-1, P5-2, P6, P7-1, P7-2, P9-1 and P9-2 (Distéfano et al., 2005, 2003; Guzmán et al., 2007; Mongelli, 2010). P5-1 has an unknown function and a vesicular-like distribution in insect cells (Maroniche et al., 2012). P5-2, P7-1 and P7-2 have nuclear localization in insect cells (Maroniche et al., 2012). MRCV P9-1 establishes cytoplasmic inclusion bodies resembling viroplasms in transfected non-host *Spodoptera frugiperda* Sf9 insect cells, has ATPase and single-stranded RNA (ssRNA) binding activities and can self-interact giving rise to homomultimers (Maroniche et al., 2011, 2010). In addition, immunoelectron microscopy assays revealed that P9-1 localizes exclusively at viroplasms within the cytoplasm of MRCV-infected plants and insect cells (Guzmán et al., 2010). These properties led us to propose P9-1 as the major matrix viroplasm protein (Maroniche et al., 2010). Finally, in insect cells,

* Corresponding author at: Instituto de Biotecnología, CICVyA, Instituto Nacional de Tecnología Agropecuaria (INTA), Nicolás Repetto y de los Reseros s/n, Hurlingham (CP 1686), Buenos Aires, Argentina.
E-mail address: delvas.mariana@inta.gob.ar (M. del Vas).

http://dx.doi.org/10.1016/j.virusres.2017.01.002
0168-1702/

MRCV P9-2 is N-glycosylated and localizes at the plasma membrane in association with filopodia-like protrusions containing actin. These features suggest P9-2 has a role in cell-to-cell movement (Maroniche et al., 2012). Interestingly, P9-2 has not been so far detected in fijivirus-infected insect or plant tissues (Isogai et al., 1998; Mao et al., 2013). During a productive infection cycle, the different structural and non-structural viral proteins are required at variable quantities and/or at different stages of infection. Accordingly, the relative mRNA expression levels of the whole fijivirus genome are known to vary at different times post-infection in plant and insect hosts (He et al., 2013). An additional strategy could rely on the regulation of viral protein turnover. PEST sequences are amino acid sequences rich in proline (P), glutamic acid (E), serine (S) and threonine (T), which serve as signals for proteolytic degradation (Rechsteiner and Rogers, 1996; Rogers et al., 1986). Many PEST-containing proteins are degraded by the ubiquitin-26S proteasome system (UPS, Rechsteiner, 1991). Interestingly, PEST-mediated protein turnover can be activated by different molecular mechanisms such as ligand binding, exposure to light and phosphorylation (Hunter, 2007; Rechsteiner and Rogers, 1996). To our understanding, the presence of functional PEST sequences has not been reported so far for any of the reovirus proteins. After an extensive screening of 100 pairs of yeast two-hybrid (Y2H) interactions between ten MRCV proteins, we showed that MRCV P6 and P9-2 can self-interact and that P6 interacts with P9-1. Interactions involving P6 and P9-1 were confirmed by bimolecular fluorescence complementation (BiFC) in plant cells. Truncated versions of P6 and P9-1 defined the regions involved in such interactions. Finally, we present evidence that the viroplasm components MRCV P9-1 and P6 contain conserved PEST sequences.

2. Materials and methods

2.1. Plasmid construction

Previously described pCR8/GW/TOPO (Invitrogen, USA) entry vectors containing MRCV NSPs P5-1, P5-2, P6, P7-1, P7-2, P9-1, P9-2 and SPs P4, P8 and P10 coding sequences (Mongelli, 2010) were used for recombination with different destination vectors listed below. These entry vectors have a stop codon and lack initiation codon. The recombinations were performed using LR Clonase II enzyme mix (Invitrogen, USA) according to the manufacturer's instructions. In addition, a new set of pCR8/GW/TOPO vectors containing the coding sequences of truncated mutants of P6 (Accession No. AAO73184.1; 788 residues) and P9-1 (Accession No. ADD71691; 337 residues) was obtained by PCR using specific primers and the previously described vectors as templates. P6DR, P6ΔDR, P6C-term and P6ΔC-term code for residues 1–105, 106-788, 450–788 and 1–449 of P6, respectively (Fig. 3A). In addition, P6ΔPEST codes for residues 50–788 of the same protein. P9-1ΔPEST lacks residues 142–153 and P9-1ΔC-arm codes for P9-1 residues 1–313. All inserts were fully sequenced before use.

For Y2H assays, the entry vectors with the MRCV coding sequences listed before were recombined into the Gateway compatible destination vectors pLAW11 and pLAW10, which express Gal4 DNA activation domain (AD) and Gal4 DNA-binding domain (BD), respectively. Prof. Dr. Richard Michelmore, from UC-Davis, kindly provided these vectors.

Plasmids used for BiFC analyses were obtained by Gateway recombination of the P6 and P9-1 entry vectors mentioned above and destination vectors pY735 and pY736, which express fusion proteins to the N- (residues 1–154) or C-terminus (residues 155–238) of fluorescent protein YFP (YFPN:X or YFPC:X), respectively (Bracha-Drori et al., 2004; Li et al., 2015a). Prof. Dr. J. Dubcovsky, from UC-Davis, kindly provided these vectors.

Plasmids used for transient expression assays in *N. benthamiana* were obtained by Gateway recombination of the P6, P9-1 and their ΔPEST mutants entry vectors into the binary destination vector pEarleyGate 203 (Earley et al., 2006). The resulting vectors express the protein of interest fused with a cMyc tag at the N-terminus. The silencing suppressor protein TBSV P19 was recombined into pEarleyGate 204 (AcV5 tag, Earley et al., 2006).

2.2. Bioinformatics sequence analysis of MRCV P6 and P9-1 proteins

Prediction of coiled-coil domains and potentially disordered regions were performed with ELM analyses tools, which comprise GlobPlot and IUPRED (disorder) and SMART/PFAM server (protein domains, Dinkel et al., 2012). Disordered regions were also analyzed with PSIPRED and DisEMBL servers (Buchan et al., 2010; Linding et al., 2003). Since no consensus has been reached about the limits of the predicted disordered region of P6, we settled a broad limit at residues 1 through 105. Prediction of PEST sequences was performed using ePESTfind (emboss.bioinformatics.nl/cgi-bin/emboss/epestfind). The ePESTfind algorithm identifies potential PEST sequences within an amino acidic sequence, and assigns a score to the prediction. Therefore, the higher the score above a threshold of +5.0 to which the algorithm assumes that the PEST sequence is biologically relevant, the higher the probability that a protein is degraded via its potential PEST sequence in eukaryotic cells (EMBOSS epestfind, 2002; Rechsteiner and Rogers, 1996). Multiple sequence alignments were performed with Clustal Omega tool of EMBL-EBI (Li et al., 2015b).

2.3. Y2H assays

Y2H assays were performed using the Matchmaker™ Gold Yeast Two-Hybrid System (Clontech, Japan) according to the manufacturer's protocol. *Saccharomyces cerevisiae* haploid strains Y187 (MATα type) and Y2H Gold (MATa mating type) were transformed with pLAW11 and pLAW10 plasmids, which express Gal4 AD:*prey* and BD:*bait* fusion proteins, by using the small-scale PEG/lithium acetate method (Gietz and Woods, 2002). Transformant yeasts were plated in synthetic defined (SD) minimal medium lacking leucine (Leu, for Y2H Gold strain transformed with BD:*bait*) or tryptophan (Trp, for Y178 strain and AD:*prey*). Co-transformants were obtained by mating according to manufacturer's indications and plated on SD-Leu-Trp, whereas MRCV-interacting proteins were selected on SD -Leu -Trp -His at 30° C for 6 days. SV-40 large T-antigen in prey vector pGADT7-T (AD:T) and murine p53 in bait vector pGBKT7-53 (BD:p53) provided in the Matchmaker kit were used as positive control and AD:T and pLAW10 empty vector (BD) were used as negative control. To rule out false positives, we co-transformed yeast cells expressing each fusion protein of interest with the corresponding AD or BD empty vectors. For autoactivation assays, yeasts transformed with AD or BD fused to the different MRCV proteins were plated in rich non-selective medium, transferred to a nitrocellulose membrane, incubated with X-gal solution (10 mg X-gal in 100 μl DMF) and the appearance of blue color was monitored over a 24 h period. For autoactivation assays of the mutant versions of P7-2, BD:P7-2^{1-152} and BD:P7-$2^{153-309}$, transformed yeasts were plated on SD −Trp 40 μg/ml X-α-Gal and 125 ng/ml Aureobasidin A and incubated at 30 °C for 3-4 days. Growth indicating antibiotic resistance and blue color appearance were monitored.

2.4. Rice protoplasts and BiFC assays

Rice japonica variety Kitaake protoplasts were prepared and transfected as described elsewhere (Bart et al., 2006). For BiFC assays, the split YFP system was used (Bracha-Drori et al., 2004).

2.5. Agroinfiltration assays

N. benthamiana plants were grown under standard greenhouse conditions at 24–26 °C, under a 14 h light/10 h dark cycle. *Agrobacterium tumefaciens* strain GV3101 carrying the different constructs was grown overnight at 28 °C on Luria-Bertani agar medium supplemented with 10 μg/ml rifampicin, 40 μg/ml gentamicin and 50 μg/ml kanamycin. Cells were pelleted, resuspended in agroinfiltration solution (10 mM $MgCl_2$, 10 mM MES and 100 μM acetosyringone) up to an optical density at 600 nm of 0.8, and incubated at room temperature for 2–4 h before infiltrating the abaxial face of the leaves. Equal volumes of agrobacteria cultures carrying the different constructs were mixed before agroinfiltration. Forty-eight h after leaf co-agroinfiltration, spots were excised and pooled in three groups (n = 3) so that each pool contained nine infiltrated spot leaves from three different plants.

2.6. Protein analyses and immunodetection

Protein extraction was performed as described previously (Isogai et al., 1998). Total proteins were quantified (Bradford, 1976) and 100 μg of total protein samples were boiled for 5 min in cracking buffer and subjected to SDS-PAGE 10%. Then, the proteins were analyzed by Western blot using an anti-cMyc mouse monoclonal primary antibody (Invitrogen, USA) and anti-mouse conjugated with alkaline phosphatase secondary antibody (Sigma-Aldrich, Germany). Detection was performed using NBT-BCIP reagents (Promega, USA). Western blot quantification was performed with ImageJ software and the ratio between cMyc antibody signal intensity and total protein load (Ponceau S stain) was calculated. Statistical significance of protein accumulation levels between cMyc:P6 or cMyc:P9-1 and their ΔPEST mutants was calculated by the unpaired *t* test using the GraphPad Prism 7 software.

2.7. Quantitative real time PCR and data analyses

Total RNA from fresh leaf tissue was extracted with Trizol reagent (Invitrogen, USA) according to the manufacturer's indications. RNA was quantified with a spectrophotometer (ThermoScientific NanoDrop™ 1000, USA) and its integrity was verified by agarose gel electrophoresis. cDNA synthesis with SuperScript™ II Reverse Transcriptase (Invitrogen, USA) was performed using 1 μg of total RNA and random primers following the manufacturer's indications. RT-qPCR experiments were carried out using the QuantiTec SYBR Green PCR kit (QIAGEN, Germany) according to the manufacturer's instructions, in an ABI7500 Real Time PCR System (Applied Biosystems, USA) with a standard program (1 min elongation time at 60 °C). Reactions were performed in a 25 μl final volume reaction with primers in a final concentration of 200 nM [for MRCV P6 forward (5′ TGGAACAGACGCGAACTTTGGT 3′, nt position 2073–2094) and reverse (5′ TGGGCAACACAAACCATAAGCG 3′, nt position 2190–2211) and for MRCV P9-1 forward (5′ GACGGCATTTTTGACCTGAT 3′, nt position 149–167) and reverse (5′ TCACGCTCAAGTGTTGGAAG 3′, nt position 232–251) and 1 μl of a 1/20 dilution of the cDNA as template. No template was added to negative control reactions. Actin was used as a reference gene (forward primer 5′ ACGCCAGTGGCCGTACAACA 3′ and reverse primer 5′ ATCGCGGACAATTTCCCGTTC 3′). Output results were exported as raw data, and introduced to the LinReg software (Ruijter et al., 2009) for baseline correction and PCR efficiency calculations. Statistical significance of Ct differences between treatments was calculated by the Mann-Whitney *t*-test using the GraphPad Prism 7software.

3. Results

3.1. Interaction screening between ten MRCV proteins by Y2H

First, we investigated the interactions between ten MRCV-coded proteins by yeast two-hybrid (Y2H) assays. This technique allows the detection of protein-protein interactions in a pair-wise manner. The two proteins (namely *bait* and *prey*) of interest are fused to the activation domain (AD) or the DNA-binding domain (BD) of the Gal 4 transcription factor and, if interaction occurs, Gal4 activates a set of reporter genes. This activation thus allows yeast to grow in SD media with Aureobasidin A, lacking Histidine (-His) or with a chromogenic substrate that confers blue color. Yeasts carrying AD:*prey* and BD:*bait* are selected in SD-Leu-Trp medium as a growth control, and if a positive protein interaction occurs they can also grow in SD-Leu-Trp-His. To rule out reporter gene activation by BD:*bait* in the absence of an interacting partner AD:*prey*, we tested autoactivation for MRCV NSPs P5-1, P5-2, P6, P7-1, P7-2, P9-1, P9-2 and SPs P4, P8 and P10 fused to the BD domain. Yeast transformed with BD:P7-2 displayed strong blue color in the presence of X-Gal (Fig. 1A). This result indicated that P7-2 acts as a transcription activation domain in this system and this protein is therefore unsuitable for Y2H analyses. We next constructed mutant versions of P7-2 containing residues 1 through 152 (P7-2^{1-152}) or 153 through 309 (P7-$2^{153-309}$), and established that the residues necessary for autoactivation are located within the first 152 amino acids of P7-2 (Fig. 1B). For this reason, we performed further Y2H assays by using BD:P7-$2^{153-309}$ truncated mutant and complete AD:P7-2.

The analysis of all possible 100 combinations revealed that P6 and P9-2 were able to self-interact (Fig. 1C and D), whereas P6 also interacted with P9-1 (Fig. 1E). As a positive control, we used the previously described MRCV P9-1 self-interaction (Maroniche et al., 2010; Fig. 1F). No false positives were detected when expressing AD:*prey* fusions with BD empty vector or expressing the opposite combination, BD:*bait* with AD empty vector. These results suggest that the previously reported P6 and P9-1 co-localizations in insect cells (Maroniche et al., 2012) are product of direct protein-protein interactions.

3.2. MRCV P6 and P9-1 interactions in plant cells using BiFC

To further confirm the interactions of P6 and P9-1 in living plant cells, we performed bimolecular fluorescence complementation (BiFC) assays in rice protoplasts. For this purpose, we obtained plasmids for protoplast transient expression that express P6 or P9-1 proteins fused downstream to the N- or C-terminal moiety of YFP, and examined reconstitution of YFP fluorescence 48 h post-co-transfection. YFP signal from P9-1 self-interaction displayed a cytoplasmic, punctuate distribution pattern typical of viroplasm inclusion bodies (VIBs, Fig. 2A). P6 self-interaction was evident, as confirmed by the observation of YFP fluorescence exclusively in the protoplast's nuclei (Fig. 2B). When we examined P6/P9-1 interaction, we detected a positive YFP signal with variable distribution depending on the constructs. For instance, YFP^N:P9-1 + YFP^C:P6 gave rise to cytoplasmic inclusion bodies of different number and sizes, whereas YFP^N:P6 + YFP^C:P9-1 interacted in the cell nucleus (Fig. 2C).

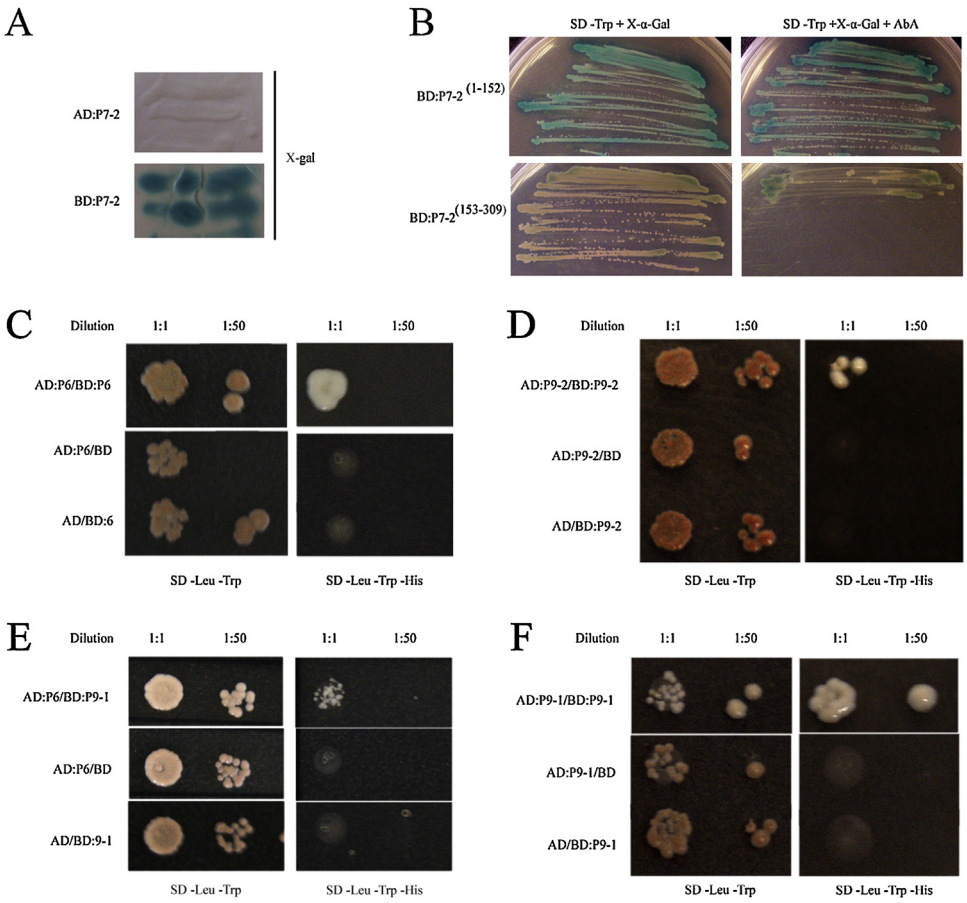

Fig. 1. Y2H interaction assay of MRCV proteins. Sequences coding for NSPs P5-1, P5-2, P6, P7-1, P7-2, P9-1 and P9-2 and SPs P4, P8 and P10 were cloned individually to obtain AD or BD fusions. A. Yeasts expressing AD:P7-2 and BD:P7-2 were transferred to a nitrocellulose membrane, incubated with X-gal and monitored for blue color appearance. B. Yeasts expressing BD:P7-2^{1-152} or BD:P7-$2^{153-309}$ were plated on SD −Trp + X-α-Gal with or without Aureobasidin (125 ng/ml AbA), in order to detect activation of reporter genes in absence of an interacting partner AD:*prey*. C to F. Co-transformants were selected in SD-Leu-Trp medium (left panels), whereas yeast expressing positive protein interactions were selected in SD-Leu-Trp-His (right panels). Yeasts were plated in 1:1 and 1:50 dilutions. Of the 100 protein-protein combinations tested, only 4 positive interactions were detected: P6/P6 (C), P9-2/P9-2 (D) P6/P9-1 (E), and P9-1/P9-1 (F). As negative controls, fusions were transformed with the corresponding empty vector (AD:prey/BD and AD/BD:bait). (For interpretation of the references to colour in this figure legend, the reader is referred to the web version of this article.)

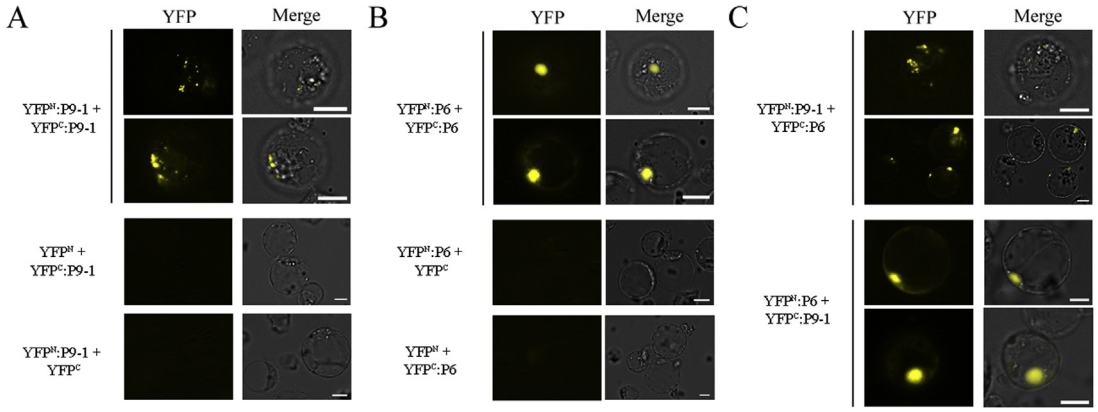

Fig. 2. BiFC assay confirms P9-1/P9-1 (A), P6/P6 (B) and P6/P9-1 (C) interactions. Rice protoplasts were transfected with the constructs indicated at the left of each image and YFP fluorescence (left panels) was observed 48 h post-transfection. As negative controls, protoplasts were transfected using either YFP^N or YFP^C empty fusions. Bright-field images were merged with YFP fluorescence images (right panels). Scale bars = 10 μm.

3.3. Identification of P6 regions involved in P6/P6 and P6/P9-1 interactions

MRCV P6 is a 90 kDa protein (Distéfano et al., 2003) with an extensive predicted coiled-coil domain at residues 560 through 619 (Maroniche et al., 2012). *In silico* analyses using ELM analyses tools showed that the N-terminal region contains a predicted disordered region (DR) spanning residues 1–105. To define the regions of P6 involved in P6/P6 and P6/P9-1 interactions, we obtained a series of truncated mutants (Fig. 3A) which were evaluated by Y2H. P6ΔDR comprised residues 106 through 788; P6DR contained only the putative DR (residues 1 through 105); P6C-term consisted of

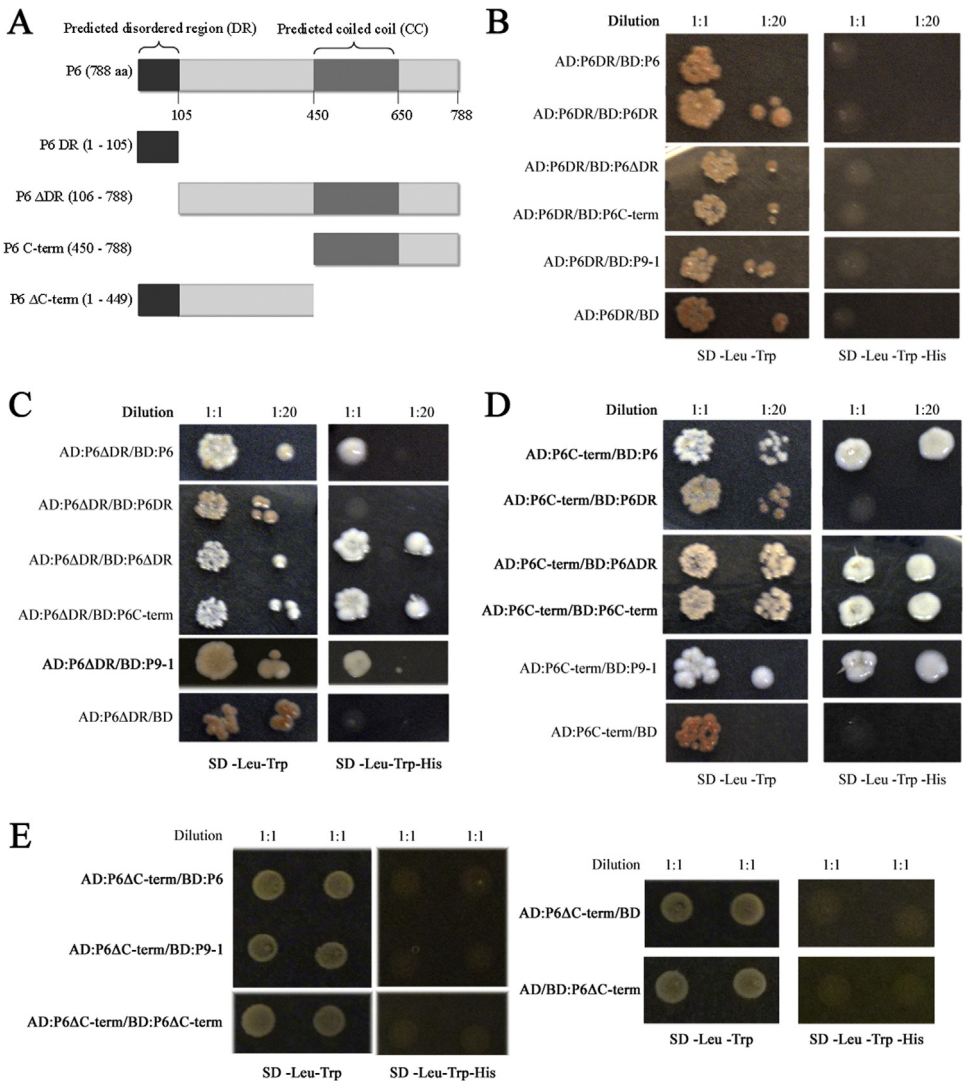

Fig. 3. Interaction analyses of P6, P9-1 and P6-derived mutants by Y2H. Schematic representation of P6 truncated mutants P6DR, P6ΔDR, P6C-term and P6ΔC-term (A). Interaction analyses of P6DR (B), P6ΔDR (C), P6 C-term (D) and P6ΔC-term (E) between P6, P9-1 and P6 truncated versions. As negative controls, fusions were transformed with the corresponding empty vector (AD:prey/BD and AD/BD:bait).

the C-terminal moiety of P6 (residues 450 through 788) including the predicted coiled-coil domain; and P6ΔC-term lacks residues 450–788. P6/P6 and P6/P9-1 interactions were not dependent on the putative disordered region, since P6DR was unable to interact with P6, P9-1 or with any of the P6-truncated mutants (Fig. 3B). In turn, P6ΔDR was able to self-interact and to interact with P6, P6C-term and P9-1 (Fig. 3C). Similarly, P6C-term was able to self-interact and to interact with P6, P6ΔDR and P9-1 (Fig. 3D). Moreover, deletion of C-term residues of P6 (P6ΔC-term) resulted in the complete loss of any interaction with P6 and P9-1, as well as of its self-interaction ability (Fig. 3E). Altogether, these results indicate that the region spanning P6 residues 450–788 is necessary and sufficient for P6/P6 and P6/P9-1 interactions.

3.4. Analysis of the contribution of P9-1 C-arm in P9-1/P9-1 and P9-1/P6 interactions

MRCV P9-1 C-terminal moiety (residues 155–337) is responsible for the formation of VIB-like structures when expressed in insect cells (Maroniche et al., 2010). *Rice black streaked dwarf virus* (RBSDV) P9-1 crystallographic structure was reported (Akita et al., 2012). In that study, Akita et al. demonstrated that RBSDV P9-1 has a protruding carboxy-terminal arm (C-arm) of 24 residues with a crucial role in the interaction of neighboring dimers to form doughnut-shaped functional octamers. To investigate if MRCV P9-1 "C-arm" was involved in P9-1/P9-1 interactions, we constructed a truncated version lacking the last 24 C-terminal residues (P9-1ΔC-arm), and by Y2H assays showed that P9-1ΔC-arm interacted with complete P9-1, but was unable to self-interact (Fig. 4A). These findings indicate that at least one C-arm is required for P9-1self-interaction. In addition, P9-1ΔC-arm was able to interact with P6, P6ΔDR and P6C-term but not with P6DR, thus indicating that the C-arm does not affect the ability of P9-1 to interact with P6 (Fig. 4B).

3.5. Identification of PEST sequences in MRCV P6 and P9-1

Before analyzing P6 and P9-1 interactions in rice protoplasts, we performed several attempts to express them transiently in *N. benthamiana* leaves by agroinfiltration. Both proteins were barely detected by Western blot only in the presence of a strong silencing suppressor such as *Tomato bushy stunt virus* P19 (Danielson and Pezacki, 2013). These pieces of evidence led us to search for degradation signals in MRCV-coded proteins. The ePESTfind algorithm identifies hydrophilic stretches with a high concentration of

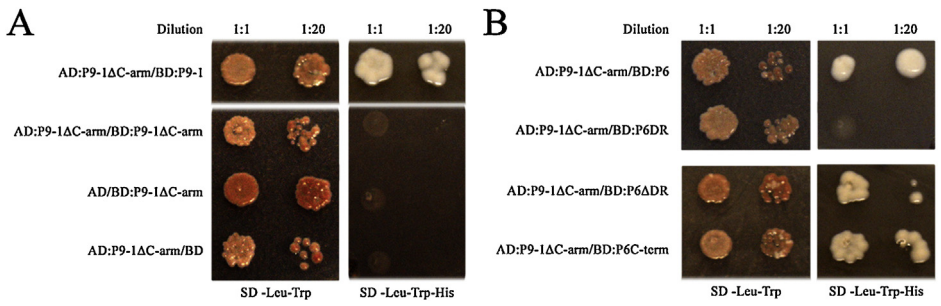

Fig. 4. Y2H interaction assays of P9-1 lacking the C-arm. The role of P9-1ΔC-arm in P9-1/P9-1 (A) and P9-1/P6 (B) interactions was tested. As negative controls, fusions were transformed with the corresponding empty vector (AD:*prey*/BD and AD/BD:*bait*).

negatively charged residues proline (P), glutamic acid (E), serine (S), and threonine (T) (EMBOSS epestfind, 2002; Rogers et al., 1986). Upon analyzing all MRCV-coded proteins, we found that only P6 and P9-1 were predicted to contain PEST sequences, in P6 residues 28–49 (PEST score: 12.23) and in P9-1 residues 142–153 (PEST score: 8.88, see Supplementary Table S1 in the online version at DOI: 10.1016/j.virusres.2017.01.002).

To explore the functionality of these predicted PEST sequences, we constructed binary vectors expressing either complete or truncated mutants, which lacked P6 residues 1–49 (P6ΔPEST) and P9-1 residues 142–153 (P9-1ΔPEST), fused to a cMyc epitope under the control of 35S promoter. These binary vectors were transiently expressed together with P19 in *N. benthamiana* leaves. Western blot analyses showed that the removal of the PEST-containing sequences significantly increased P6 and P9-1 accumulation when compared to the full version of the proteins (p-values < 0.05, Fig. 5). All qPCR analyses of agroinfiltrated tissue showed no significant differences (p-values > 0.05) between mRNA levels coding for P6 or P9-1 and their ΔPEST mutants (see Supplementary Fig. S1 in the online version at DOI: 10.1016/j.virusres.2017.01.002), thus indicating that the observed differences in protein accumulation were due to a post-transcriptional process.

We then analyzed whether the presence of PEST sequences is conserved in the genus *Fijivirus*. For this purpose, we performed multiple sequence alignments of MRCV P6 and P9-1 homologous protein sequences of RBSDV, *Southern rice black streaked dwarf virus* (SRBSDV), *Maize rough dwarf virus* (MRDV), *Fiji disease virus* (FDV) and *Nilaparvata lugens reovirus* (NLRV) and analyzed them with the ePESTfind algorithm (Fig. 6 and Supplementary Table S1 in the online version at DOI: 10.1016/j.virusres.2017.01.002). The presence of PEST sequences, which located at the N-terminal region, was conserved amongst all fijivirus P6 proteins. Noticeably, as in MRCV P6, the N-terminal regions of all fijivirus counterparts contain as well residues predicted to be disordered (data not shown). In turn, P9-1 PEST sequences were relatively less conserved, since they were present only in MRCV, RBSDV and MRDV.

4. Discussion

The aim of this work was to analyze the interactions between MRCV proteins to further characterize their functional roles. We performed Y2H analysis to evaluate possible interactions between ten MRCV NSPs and SPs, and identified that P6 self-interacted and also interacted with P9-1. The BiFC experiments in rice protoplasts confirmed these interactions. BiFC allows the identification of protein-protein interactions and, although this technique was not intended for the study of subcellular distribution, it was somehow surprising to detect P6/P6 and P6/P9-1 interactions occurring at the protoplast's nuclei. YFP N- and C-terminal fusions to P6 or P9-1 result in proteins that are larger than the size-exclusion limit of the nuclear pore complexes (Hoelz et al., 2011). Thus, an active import process should be required for entering the nuclei. As previously reported in Maroniche et al. (2012), the non-structural MRCV proteins P5-2, P7-1 and P7-2 display nuclear localization when transiently expressed in *Spodoptera frugiperda* Sf9 insect cells; however, this was not observed for P6 or P9-1. Moreover, P9-1 has been detected exclusively at viroplasms within the cytoplasm of MRCV-infected plants and insect cells by immunoelectron microscopy assays (Guzmán et al., 2010), whereas P6 distribution in MRCV-infected plants and insects remains unknown.

Aminev et al. (2003a, 2003b) have peviously described nuclear localizations and functions of proteins encoded by RNA viruses that are considered to replicate in the cytoplasm. Interestingly, novel conformational signals for nuclear localization (Audsley et al., 2016) could arise after dimer formation. In addition, matrix proteins of negative-sense RNA viruses with critical roles in cytoplasmic replication and virus assembly have also been detected at the nucleus of infected cells (as reviewed by Audsley et al., 2016). More studies will be required to explore the possible implications of a putative nuclear localization of P6/P6 complexes during the infection cycle.

In the case of P6/P9-1 protein interactions, nuclear localization depended on the constructions employed. While YFP^N:P9-1 + YFP^C:P6 localized in cytoplasmic inclusion bodies resembling viroplasms, YFP^N:P6 + YFP^C:P9-1 interacted in the cell nucleus. We have previously observed that subcellular localizations can vary depending on the plasmids and fusion constructs employed (Maroniche et al., 2012). Therefore, we interpret this BiFC result as a confirmation of P6/P9-1 protein interaction but further studies will be needed to confirm the subcellular distribution observed.

Additionally, BiFC assays showed that P9-1 self-interacts to form a punctuate cytoplasmic distribution, as previously shown in insect cells (Maroniche et al., 2012), further confirming P9-1 role as the major MRCV viroplasm component in plant cells (Guzmán et al., 2010; Maroniche et al., 2012, 2010). P6 is proposed to be a minor viroplasm protein because it is redirected towards P9-1 VIBs-like structures when these two proteins are co-expressed in insect cells (Maroniche et al., 2012). The present results are in agreement with these previous findings, and suggest that the co-localization observed in insect cells occur as a result of direct protein-protein interactions.

The crystallographic analysis of RBSDV P9-1 showed that this protein contains a carboxyl-terminus C-arm that is necessary for the formation of functional octamers; and the deletion of this C-arm results in the absence of VIBs-like structures, although dimer formation is not impaired (Akita et al., 2012). By performing Y2H analysis, we demonstrated that MRCV P9-1 dimers can be formed only when at least one C-arm is present in this interaction, thus suggesting an essential role of this structure in the formation of VIBs.

By using a series of truncated mutants, we determined that the C-terminal moiety of P6 (residues 450–788), which contains

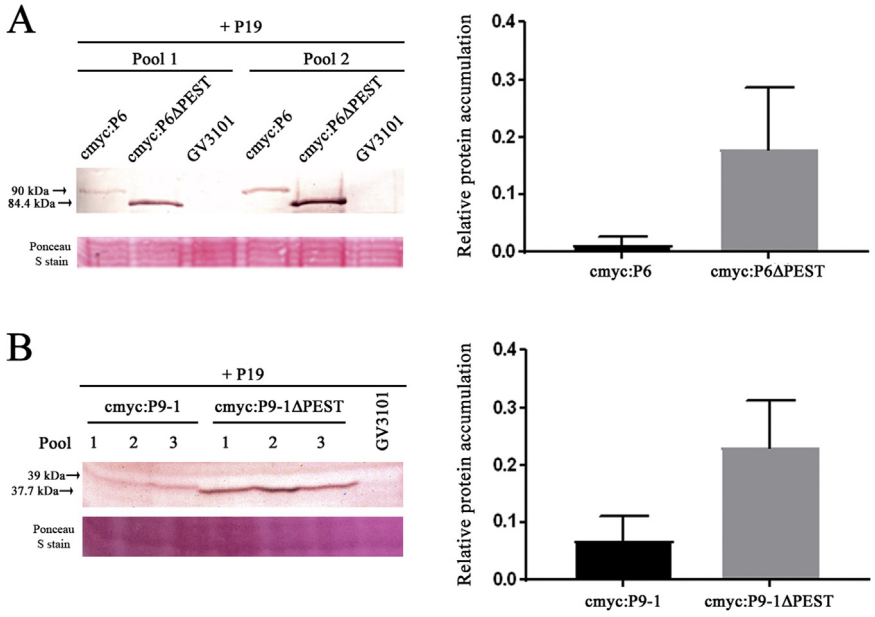

Fig. 5. PEST sequences destabilize P6 and P9-1 in *N. benthamiana*. cMyc:P6 or cMyc:P6ΔPEST (A), and cMyc:P9-1 or cMyc:P9-1 ΔPEST (B) were expressed by agroinfiltration in *N. benthamiana* leaves. *A. tumefaciens* GV3101 was used as a mock control. Agroinfiltration assays were performed in the presence of TBSV P19 suppressor of gene silencing. Samples were pooled (n = 3); total protein was extracted and subjected to SDS-PAGE and to Western blot analyses with anti-cMyc antibody (left panels). Protein accumulation levels of P6 or P9-1 and their ΔPEST mutants relative to GV3101 and to total protein load (shown as Ponceau S stain) were quantified (right panels). Then, a statistical analysis was performed by an unpaired *t* test. Bars represent standard error of the mean (SEM).

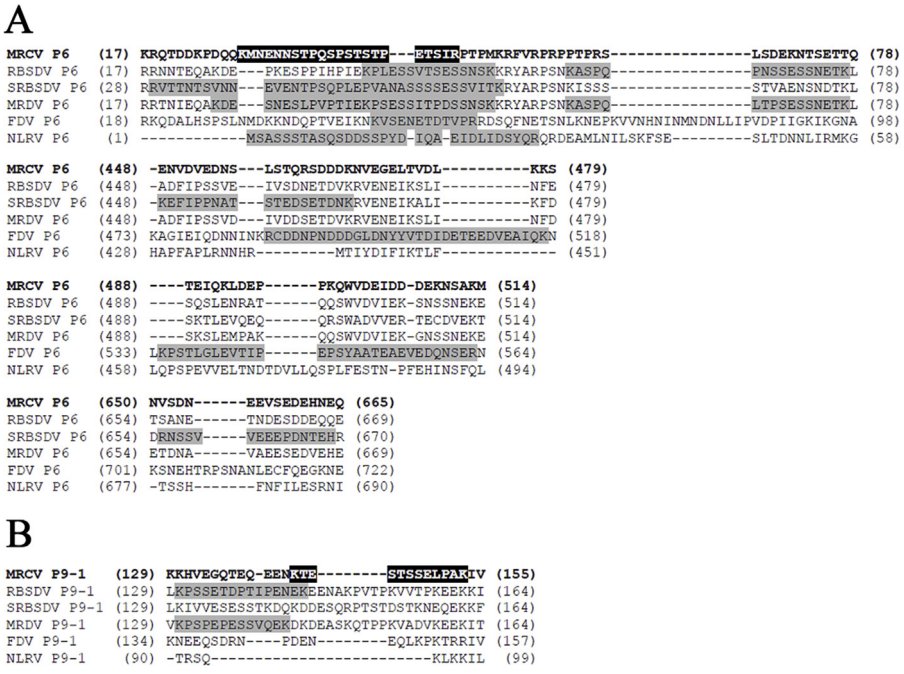

Fig. 6. Conservation analysis of PEST sequences among P6 (A) and P9-1 (B) fijivirus proteins. Multiple sequence alignment of fijivirus P6 and P9-1 proteins was performed with CLUSTAL Omega tool. MRCV sequences are marked in bold and their potential PEST sequences are highlighted in black, whereas the PEST sequences identified for other fijiviruses are highlighted in gray. MRCV, *Mal de Río Cuarto virus*; RSBDV, *Rice black streaked dwarf virus*; SRBSDV, *Southern rice black streaked dwarf virus*; MRDV, *Maize rough dwarf virus*; FDV, *Fiji disease virus*; NLRV, *Nilaparvata lugens reovirus*.

a predicted coiled-coil domain (position 450–650), is necessary and sufficient for P6/P6 and P6/P9-1 interactions. Furthermore, the deletion of the P9-1C-arm does not seem to affect P6/P9-1 interaction. The ability of P6 to self-interact and to interact with P9-1 has also been reported for other fijiviruses such as RBSDV (Sun et al., 2013; Wang et al., 2011) and SRBSDV (J. Li et al., 2014; Mao et al., 2013). Nevertheless, the regions involved in P6 and P9-1 interactions are not necessarily the same for all three fijiviruses. As in the case of MRCV, RBSDV P6 central region (residues 400–675, which also contain a putative coiled-coil) is necessary for self-interaction and P6/P9-1 interaction. However, full-length RBSDV P9-1 may also be essential for P6/P9-1 interaction, as all P9-1 mutants tested abolished such interaction (Wang et al., 2011). Unlike MRCV P6, full-length SRBSDV P6 is needed for self-interaction, whereas residues 1–93 of P6 and full-length P9-1 are required for SRBSDV P6/P9-1 interaction (J. Li et al., 2014). Taken together, these results

demonstrate that, despite sharing general characteristics, the P6 and P9-1 proteins of each fijivirus have unique and specific features, therefore highlighting the importance of a detailed study on each virus species.

The Y2H assays also revealed that P9-2 can self-interact *in vivo*. This interaction might be important for the formation of filopodia-like protrusions of the cell membrane that are observed upon expression of P9-2 in Sf9 insect cells (Maroniche et al., 2012).

Full-length MRCV P7-2 conferred autoactivation of the Y2H reporter genes, thus indicating that P7-2 can act as a transcriptional activation domain. Furthermore, this protein occasionally displays nuclear localization, when expressed in insect Sf9 cells (Maroniche et al., 2012). Taken together, it is tempting to speculate that P7-2 could regulate host gene expression during infection.

Viroplasms are very dynamic structures where viral protein synthesis, viral genome replication and viral progeny assembly take place. They are composed by one or two non-structural major proteins, viral RNA and other minor viral proteins (structural and non-structural) (Antczak and Joklik, 1992; Brookes et al., 1993), as well as cellular host proteins (Broering et al., 2004; Cabral-Romero and Padilla-Noriega, 2006; Eaton et al., 1987; Parker et al., 2002). As observed for rotavirus, at early time points viroplasms are detected as punctuate, discrete cytoplasmic inclusions whose number first increases, and then decreases as viroplasms start to fuse during the infection (Eichwald et al., 2004). For SRBSDV, the model proposed for viroplasm maturation involves the existence of two distinct regions: a granular region predominantly formed by P9-1, where viral replication takes place and a surrounding fibrillar region mainly composed of P5, where viral packaging occurs. In both cases, P6 is a minor component (Mao et al., 2013). Such dynamic process would require a tight regulation of viral protein expression.

Indeed, the ubiquitin 26S-proteasome system (UPS) plays an important role in virus-host interactions (Alcaide-Loridan and Jupin, 2012; Dielen et al., 2010; Luo, 2016). Specific to the *Reoviridae* family, both rotavirus and avian reovirus replication and viroplasm formation require a functional proteasome. Treatment with proteasome inhibitors impairs viral protein synthesis, viroplasm formation and viral genome replication (Chen et al., 2008; Contin et al., 2011; Lopez et al., 2011). Interestingly, for *Rotavirus*, the assembly of new viroplasms is impaired by blocking proteasome activity (Contin et al., 2011). In *Bluetongue virus,* inhibition of the proteasome leads to decreased virus titers and viral protein synthesis (Bhattacharya et al., 2015).

Although transient expression in *N. benthamiana* proved to be useful for studying fijivirus viroplasm components (J. Li et al., 2014, 2013; Songbai et al., 2013), we failed to express sufficient amounts of MRCV P6 and P9-1 in this model system. In agreement, Wang et al. (2011) also encountered problems trying to express complete RBSDV P6 fused to DsRed in *N. benthamiana* (Wang et al., 2011). In our study, both MRCV P6 and P9-1 contain conserved PEST sequences that are absent in the rest of MRCV proteins. To date, few studies report on viruses regulating their protein expression through PEST sequences. For instance, the RNA polymerase RNA-dependent 66 K of *Turnip yellow mosaic virus* (TYMV) contains a PEST sequence that mediates degradation by the UPS (Camborde et al., 2010; Drugeon and Jupin, 2002; Hericourt et al., 2000), and is also phosphorylated within the PEST sequence (Jakubiec et al., 2006). *Cauliflower mosaic virus* (CaMV) capsid protein p44 and *Potato virus X* TGBp1 movement protein also contain functional PEST sequences (Binaghi, 2012; Karsies et al., 2001). Bovine papillomavirus E2 protein contains a PEST sequence within a disordered region that can be phosphorylated, thus accelerating E2 degradation by the UPS. A change in conformational stability, rather than recognition of a phosphate modification, may modulate the degradation of this protein by the UPS (García-Alai et al., 2006; Penrose and McBride, 2000). Remarkably, the MRCV P6 PEST sequence is located within a predicted disordered region at the N-terminus of the protein. Given that disordered regions do not adopt a stable conformation, they can contain readily accessible linear motifs (Linding et al., 2003).

Considering these results, we propose that P6 and P9-1 PEST sequences can have a regulatory role in viroplasm dynamics. Interestingly, all five serines (at positions 34, 38, 40, 42 and 47) and threonine 43 within the MRCV P6 PEST sequence, as well as serines at position 145, 157 and 148 and threonine 146 of P9-1 PEST are predicted to be possible phosphorylation sites (data not shown). The discovery of PEST-containing proteins in members of the *Reoviridae* family may contribute to the understanding of viroplasm dynamics in different genera of this virus family.

Acknowledgments

This work was supported by Research project PE AEBIO-1131023 from the National Institute of Agronomic Technology (INTA) and by PICT 2012 N 0391 from the National Agency for the Promotion of Science and Technology (ANPCyT). MdV and VA are Researchers from the Consejo Nacional de Investigaciones Científicas y Técnicas (CONICET). LdH holds a fellowship from CONICET. The authors would like to specially thank to Prof. Dr. Jorge Dubcovsky, Dr. Huiqiong Lin and Chengxia Li for kindly providing plasmids and for assistance in the BiFC assays, Prof. Dr. Richard Michelmore for kindly providing plasmids, Dr. Julia Sabio y García for English language editing, and Laura Inés Ramos for excellent technical assistance.

References

Akita, F., Higashiura, A., Shimizu, T., Pu, Y., Suzuki, M., Uehara-Ichiki, T., Sasaya, T., Kanamaru, S., Arisaka, F., Tsukihara, T., Nakagawa, A., Omura, T., 2012. Crystallographic analysis reveals octamerization of viroplasm matrix protein P 9-1 of Rice black streaked dwarf virus. J. Virol. 86, 746–756, http://dx.doi.org/10.1128/JVI.00826-11.

Alcaide-Loridan, C., Jupin, I., 2012. Ubiquitin and plant viruses, let's play together! Plant Physiol. 160, 72–82, http://dx.doi.org/10.1104/pp.112.201905.

Aminev, A.G., Amineva, S.P., Palmenberg, A.C., 2003a. Encephalomyocarditis virus (EMCV) proteins 2A and 3BCD localize to nuclei and inhibit cellular mRNA transcription but not rRNA transcription. Virus Res. 95, 59–73, http://dx.doi.org/10.1016/S0168-1702(03)00163-1.

Aminev, A.G., Amineva, S.P., Palmenberg, A.C., 2003b. Encephalomyocarditis viral protein 2A localizes to nucleoli and inhibits cap-dependent mRNA translation. Virus Res. 95, 45–57, http://dx.doi.org/10.1016/S0168-1702(03)00162-X.

Antczak, J.B., Joklik, W.K., 1992. Reovirus genome segment assortment into progeny genomes studied by the use of monoclonal antibodies directed against reovirus proteins. Virology 187, 760–776.

Arneodo, J.D., Guzman, F.A., Conci, L.R., Laguna, I.G., Truol, G.A., 2002. Transmission features of Mal de Río Cuarto virus in wheat by its planthopper vector Delphacodes kuscheli. Ann. Appl. Biol. 141, 195–200.

Attoui, H., Mertens, P.P.C., Becnel, J., Belaganahalli, S., Bergoin, M., Brussaard, C.P., Chappell, J.D., Ciarlet, M., del Vas, M., Dermody, T.S., Dormitzer, P.R., Duncan, R., Fang, Q., Graham, R., Guglielmi, K.M., Harding, R.M., Hillman, B., Makkay, A., Marzachì, C., Matthijnssens, J., Milne, R.G., Mohd Jaafar, F., Mori, H., Noordeloos, A.A., Omura, T., Patton, J.T., Rao, S., Maan, M., Stoltz, D., Suzuki, N., Upadhyaya, N.M., Wei, C., Zhou, H., 2011. Family Reoviridae. In: King, A.M.Q., Adams, M.J., Castens, E.B., Lefkowitz, E.J. (Eds.), Virus Taxonomy. Ninth Report of The International Comittee on Taxonomy of Viruses. Elsevier, San Diego, pp. 541–638.

Audsley, M.D., Jans, D.A., Moseley, G.W., 2016. Roles of nuclear trafficking in infection by cytoplasmic negative-strand RNA viruses: paramyxoviruses and beyond. J. Gen. Virol. 97, 2463–2481, http://dx.doi.org/10.1099/jgv.0.000575.

Bart, R., Chern, M., Park, C.J., Bartley, L., Ronald, P.C., 2006. A novel system for gene silencing using siRNAs in rice leaf and stem-derived protoplasts. Plant Methods 2, 13, http://dx.doi.org/10.1186/1746-4811-2-13.

Bhattacharya, B., Celma, C.C., Roy, P., 2015. Influence of cellular trafficking pathway on bluetongue virus infection in ovine cells. Viruses 7, 2378–2403, http://dx.doi.org/10.3390/v7052378.

Binaghi, M., 2012. Rol de la fosforilación en la regulación funcional de la proteína de movimiento TGBp1 del Potato virus X. Inst. Investig. en Ing. Genética y Biol. Mol. Fac. Ciencias Exactas y Nat. Universidad de Buenos Aires, Buenos Aires.

Bracha-Drori, K., Shichrur, K., Katz, A., Oliva, M., Angelovici, R., Yalovsky, S., Ohad, N., 2004. Detection of protein-protein interactions in plants using bimolecular

fluorescence complementation. Plant J. 40, 419–427, http://dx.doi.org/10.1111/j.1365-313X.2004.02206.x.
Bradford, M.M., 1976. A rapid and sensitive method for the quantitation of protein utilizing the principle of protein-dye binding. Anal. Biochem. 72, 248–254, http://dx.doi.org/10.1016/0003-2697(76)90527-3.
Broering, T.J., Kim, J., Miller, C.L., Piggott, C.D., Dinoso, J.B., Nibert, M.L., Parker, J.S., 2004. Reovirus nonstructural protein mu NS recruits viral core surface proteins and entering core particles to factory-like inclusions. J. Virol. 78, 1882–1892.
Brookes, S.M., Hyatt, A.D., Eaton, B.T., 1993. Characterization of virus inclusion bodies in bluetongue virus-infected cells. J. Gen. Virol. 74 (Pt 3), 525–530.
Buchan, D.W., Ward, S.M., Lobley, A.E., Nugent, T.C., Bryson, K., Jones, D.T., 2010. Protein annotation and modelling servers at University College London. Nucleic Acids Res. 38, W563–W568, http://dx.doi.org/10.1093/nar/gkq427.
Cabral-Romero, C., Padilla-Noriega, L., 2006. Association of rotavirus viroplasms with microtubules through NSP2 and NSP5. Mem. Inst. Oswaldo Cruz 101, 603–611.
Camborde, L., Planchais, S., Tournier, V., Jakubiec, A., Drugeon, G., Lacassagne, E., Pflieger, S., Chenon, M., Jupin, I., 2010. The ubiquitin-proteasome system regulates the accumulation of Turnip yellow mosaic virus RNA-dependent RNA polymerase during viral infection. Plant Cell 22, 3142–3152, http://dx.doi.org/10.1105/tpc.109.072090.
Chen, Y.T., Lin, C.H., Ji, W.T., Li, S.K., Liu, H.J., 2008. Proteasome inhibition reduces avian reovirus replication and apoptosis induction in cultured cells. J. Virol. Methods 151, 95–100, http://dx.doi.org/10.1016/j.jviromet.2008.03.016.
Contin, R., Arnoldi, F., Mano, M., Burrone, O.R., 2011. Rotavirus replication requires a functional proteasome for effective assembly of viroplasms. J. Virol. 85, 2781–2792, http://dx.doi.org/10.1128/JVI.01631-10.
Danielson, D.C., Pezacki, J.P., 2013. Studying the RNA silencing pathway with the p19 protein. FEBS Lett., http://dx.doi.org/10.1016/j.febslet.2013.01.036.
Dielen, A.S., Badaoui, S., Candresse, T., German-Retana, S., 2010. The ubiquitin/26S proteasome system in plant-pathogen interactions: a never-ending hide-and-seek game. Mol. Plant Pathol., http://dx.doi.org/10.1111/j.1364-3703.2009.00596.x.
Dinkel, H., Michael, S., Weatheritt, R.J., Davey, N.E., Van Roey, K., Altenberg, B., Toedt, G., Uyar, B., Seiler, M., Budd, A., Jodicke, L., Dammert, M.A., Schroeter, C., Hammer, M., Schmidt, T., Jehl, P., McGuigan, C., Dymecka, M., Chica, C., Luck, K., Via, A., Chatr-Aryamontri, A., Haslam, N., Grebnev, G., Edwards, R.J., Steinmetz, M.O., Meiselbach, H., Diella, F., Gibson, T.J., 2012. ELM–the database of eukaryotic linear motifs. Nucleic Acids Res. 40, D242–D251, http://dx.doi.org/10.1093/nar/gkr1064.
Distéfano, A.J., Conci, L.R., Munoz Hidalgo, M., Guzmán, F.A., Hopp, H.E., del Vas, M., 2002. Sequence analysis of genome segments S4 and S8 of Mal de Rio Cuarto virus (MRCV): evidence that the virus should be a separate Fijivirus species. Arch. Virol 147, 1699–1709.
Distéfano, A.J., Conci, L.R., Muñoz Hidalgo, M., Guzmán, F.A., Hopp, H.E., del Vas, M., 2003. Sequence and phylogenetic analysis of genome segments S1, S2, S3 and S6 of Mal de Rio Cuarto virus, a newly accepted Fijivirus species. Virus Res. 92, 113–121.
Distéfano, A.J., Hopp, H.E., del Vas, M., 2005. Sequence analysis of genome segments S5 and S10 of Mal De Rio Cuarto virus (*Fijivirus, Reoviridae*). Arch. Virol. 150, 1241–1248.
Distéfano, A.J., Maldonado, S., Hopp, H.E., del Vas, M., 2009. Mal de Rio Cuarto virus (MRCV) genomic segment S3 codes for the major core capsid protein. Virus Genes 38, 455–460.
Drugeon, G., Jupin, I., 2002. Stability in vitro of the 69 K movement protein of Turnip yellow mosaic virus is regulated by the ubiquitin-mediated proteasome pathway. J. Gen. Virol. 83, 3187–3197.
EMBOSS epestfind [WWW Document], 2002. URL http://emboss.bioinformatics.nl/cgi-bin/emboss/help/epestfind.
Earley, K.W., Haag, J.R., Pontes, O., Opper, K., Juehne, T., Song, K., Pikaard, C.S., 2006. Gateway-compatible vectors for plant functional genomics and proteomics. Plant J. 45, 616–629, http://dx.doi.org/10.1111/j.1365-313X.2005.02617.x.
Eaton, B.T., Hyatt, A.D., White, J.R., 1987. Association of bluetongue virus with the cytoskeleton. Virology 157, 107–116.
Eichwald, C., Rodriguez, J.F., Burrone, O.R., 2004. Characterization of rotavirus NSP2/NSP5 interactions and the dynamics of viroplasm formation. J. Gen. Virol. 85, 625–634.
Firth, A.E., Atkins, J.F., 2009. Analysis of the coding potential of the partially overlapping 3' ORF in segment 5 of the plant fijiviruses. Virol. J. 6, 32.
García-Alai, M.M., Gallo, M., Salame, M., Wetzler, D.E., McBride, A.A., Paci, M., Cicero, D.O., de Prat-Gay, G., 2006. Molecular basis for phosphorylation-dependent, PEST-mediated protein turnover. Structure 14, 309–319, http://dx.doi.org/10.1016/j.str.2005.11.012.
Gietz, R.D., Woods, R.A., 2002. Transformation of yeast by lithium acetate/single-stranded carrier DNA/polyethylene glycol method. Methods Enzymol., http://dx.doi.org/10.1016/S0076-6879(02)50957-5.
Guzmán, F.A., Distéfano, A.J., Arneodo, J.D., Hopp, H.E., Lenardón, S.L., del Vas, M., Conci, L.R., 2007. Sequencing of the bicistronic genome segments S7 and S9 of Mal de Rio Cuarto virus (Fijivirus, Reoviridae) completes the genome of this virus. Arch. Virol 152, 565–573.
Guzmán, F.A., Arneodo, J.D., Saavedra Pons, A.B., Truol, G.A., Luque, A.V., Conci, L.R., 2010. Immunodetection and subcellular localization of Mal de Rio Cuarto virus P 9-1 protein in infected plant and insect host cells. Virus Genes 41, 111–117, http://dx.doi.org/10.1007/s11262-010-0480-9.
He, P., Liu, J., He, M., Wang, Z., Chen, Z., Guo, R., Correll, J.C., Yang, S., 2013. Quantitative detection of relative expression levels of the whole genome of Southern rice black-streaked dwarf virus and its replication in different hosts. Virol. J. 10, 1–9.
Hericourt, F., Blanc, S., Redeker, V., Jupin, I., 2000. Evidence for phosphorylation and ubiquitinylation of the turnip yellow mosaic virus RNA-dependent RNA polymerase domain expressed in a baculovirus-insect cell system. Biochem. J. 349, 417–425.
Hoelz, A., Debler, E.W., Blobel, G., 2011. The structure of the nuclear pore complex. Annu. Rev. Biochem. 80, 613–643, http://dx.doi.org/10.1146/annurev-biochem-060109-151030.
Hunter, T., 2007. The age of crosstalk: phosphorylation ubiquitination, and beyond. Mol. Cell 28, 730–738, http://dx.doi.org/10.1016/j.molcel.2007.11.019.
Isogai, M., Uyeda, I., Lee, B.C., 1998. Detection and assignment of proteins encoded by rice black streaked dwarf fijivirus S7, S8, S9 and S10. J. Gen. Virol. 79 (Pt 6), 1487–1494.
Jakubiec, A., Tournier, V., Drugeon, G., Pflieger, S., Camborde, L., Vinh, J., Héricourt, F., Redeker, V., Jupin, I., 2006. Phosphorylation of viral RNA-dependent RNA polymerase and its role in replication of a plus-strand RNA virus. J. Biol. Chem. 281, 21236–21249, http://dx.doi.org/10.1074/jbc.M600052200.
Karsies, A., Hohn, T., Leclerc, D., 2001. Degradation signals within both terminal domains of the cauliflower mosaic virus capsid protein precursor. Plant J. 27, 335–343, http://dx.doi.org/10.1046/j.1365-313x.2001.01093.x.
Lenardón A., Giolitti, F., March, G.J. y Nome, S. F., S.L. R., 1998. Virus del Mal de Río Cuarto: Estudios de transmisión por semilla. RIA 99 a105.
Li, J., Xue, J., Zhang, H.M., Yang, J., Lv, M.F., Xie, L., Meng, Y., Li, P.P., Chen, J.P., 2013. Interactions between the P6 and P 5-1 proteins of southern rice black-streaked dwarf fijivirus in yeast and plant cells. Arch. Virol. 158, 1649–1659, http://dx.doi.org/10.1007/s00705-013-1660-4.
Li, J., Xue, J., Zhang, H.M., Yang, J., Xie, L., Chen, J.P., 2014. Characterization of homologous and heterologous interactions between viroplasm proteins P6 andof the fijivirus southern rice black-streaked dwarf virus. Arch. Virol., 1–9, http://dx.doi.org/10.1007/s00705-014-2268-z.
Li, C., Lin, H., Dubcovsky, J., 2015a. Factorial combinations of protein interactions generate a multiplicity of florigen activation complexes in wheat and barley. Plant J. 84, 70–82, http://dx.doi.org/10.1111/tpj.12960.
Li, W., Cowley, A., Uludag, M., Gur, T., McWilliam, H., Squizzato, S., Park, Y.M., Buso, N., Lopez, R., 2015b. The EMBL-EBI bioinformatics web and programmatic tools framework. Nucleic Acids Res. 43, W580–W584, http://dx.doi.org/10.1093/nar/gkv279.
Linding, R., Russell, R.B., Neduva, V., Gibson, T.J., 2003. GlobPlot: exploring protein sequences for globularity and disorder. Nucleic Acids Res. 31, 3701–3708.
Lopez, T., Silva-Ayala, D., Lopez, S., Arias, C.F., 2011. Replication of the rotavirus genome requires an active ubiquitin-proteasome system. J. Virol. 85, 11964–11971, http://dx.doi.org/10.1128/JVI.05286-11.
Luo, H., 2016. Interplay between the virus and the ubiquitin-proteasome system: molecular mechanism of viral pathogenesis. Curr. Opin. Virol. 17, 1–10, http://dx.doi.org/10.1016/j.coviro.2015.09.005.
Mao, Q., Zheng, S., Han, Q., Chen, H., Ma, Y., Jia, D., Chen, Q., Wei, T., 2013. New model for the genesis and maturation of viroplasms induced by fijiviruses in insect vector cells. J. Virol. 87, 6819–6828, http://dx.doi.org/10.1128/JVI.00409-13.
Maroniche, G.A., Mongelli, V.C., Peralta, A.V., Distéfano, A.J., Llauger, G., Taboga, O.A., Hopp, E.H., del Vas, M., 2010. Functional and biochemical properties of Mal de Río Cuarto virus (Fijivirus, Reoviridae) P 9-1 viroplasm protein show further similarities to animal reovirus counterparts. Virus Res. 152, 96–103, http://dx.doi.org/10.1016/j.virusres.2010.06.010.
Maroniche, G.A., Mongelli, V.C., Alfonso, V., Llauger, G., Taboga, O., del Vas, M., 2011. Development of a novel set of Gateway-compatible vectors for live imaging in insect cells. Insect Mol. Biol. 20, 675–685, http://dx.doi.org/10.1111/j.1365-2583.2011.01100.x.
Maroniche, G.A., Mongelli, V.C., Llauger, G., Alfonso, V., Taboga, O., del Vas, M., 2012. In vivo subcellular localization of Mal de Río Cuarto virus (MRCV) non-structural proteins in insect cells reveals their putative functions. Virology 430, 81–89, http://dx.doi.org/10.1016/j.virol.2012.04.016.
Mongelli, V.C., 2010. Estudio funcional de las proteínas codificadas por el virus del Mal de Río Cuarto en hospedantes vegetales. Fac. Ciencias Exactas y Nat. Universidad de Buenos Aires, Buenos Aires.
Parker, J.S., Broering, T.J., Kim, J., Higgins, D.E., Nibert, M.L., 2002. Reovirus core protein mu2 determines the filamentous morphology of viral inclusion bodies by interacting with and stabilizing microtubules. J. Virol. 76, 4483–4496.
Penrose, K.J., McBride, A.A., 2000. Proteasome-mediated degradation of the papillomavirus E2-TA protein is regulated by phosphorylation and can modulate viral genome copy number. J. Virol. 74, 6031–6038.
Rechsteiner, M., Rogers, S.W., 1996. PEST sequences and regulation by proteolysis. Trends Biochem. Sci. 21, 267–271, http://dx.doi.org/10.1016/0092-8674(91)90104-7.
Rechsteiner, M., 1991. Natural substrates of the ubiquitin proteolytic pathway. Cell 66, 615–618, http://dx.doi.org/10.1016/0092-8674(91)90104-7.
Rogers, S., Wells, R., Rechsteiner, M., 1986. Amino acid sequences common to rapidly degraded proteins: the PEST hypothesis. Science 234, 364–368, http://dx.doi.org/10.1126/science.2876518 (80).
Ruijter, J.M., Ramakers, C., Hoogaars, W.M., Karlen, Y., Bakker, O., van den Hoff, M.J., Moorman, A.F., 2009. Amplification efficiency: linking baseline and bias in the analysis of quantitative PCR data. Nucleic Acids Res. 37, e45.
Songbai, Z., Zhenguo, D., Liang, Y., Zhengjie, Y., Kangcheng, W., Guangpu, L., Zujian, W., Lianhui, X., 2013. Identification and characterization of the interaction between viroplasm-associated proteins from two different plant-infecting

reoviruses and eEF-1A of rice. Arch. Virol 158, 2031–2039, http://dx.doi.org/10.1007/s00705-013-1703-x.
Sun, L., Xie, L., Andika, I.B., Tan, Z., Chen, J., 2013. Non-structural protein P6 encoded by rice black-streaked dwarf virus is recruited to viral inclusion bodies by binding to the viroplasm matrix protein P 9-1. J. Gen. Virol. 94, 1908–1916, http://dx.doi.org/10.1099/vir.0.051698-0.
Supyani, S., Hillman, B.I., Suzuki, N., 2007. Baculovirus expression of the 11 mycoreovirus-1 genome segments and identification of the guanylyltransferase-encoding segment. J. Gen. Virol. 88, 342–350.
Wang, Q., Tao, T., Zhang, Y., Wu, W., Li, D., Yu, J., Han, C., 2011. Rice black-streaked dwarf virus P6 self-interacts to form punctate, viroplasm-like structures in the cytoplasm and recruits viroplasm-associated protein P 9-1. Virol. J. 8, 24, http://dx.doi.org/10.1186/1743-422X-8-24.
World of Corn, 2016. World Corn Imports/Exports 2015–2016 [WWW Document]. URL www.worldofcorn.com/#world-corn-exports-imports.
de Remes Lenicov, A.M., Teson, A., Dagoberto, E., Huguet, N., 1985. Hallazgo de uno de los vectores del Mal de Río Cuarto en maíz. Gac. Agropecu. 25, 251–258.